


RESEARCH

Open Access



# An allosteric interleukin-1 receptor modulator mitigates inflammation and photoreceptor toxicity in a model of retinal degeneration

Rabah Dabouz<sup>1,2,3</sup>, Colin W. H. Cheng<sup>1,2,3</sup>, Pénélope Abram<sup>2</sup>, Samy Omri<sup>2</sup>, Gael Cagnone<sup>3</sup>, Khushnouma Virah Sawmy<sup>3</sup>, Jean-Sébastien Joyal<sup>3</sup>, Michel Desjarlais<sup>2</sup>, David Olson<sup>4</sup>, Alexander G. Weil<sup>5</sup>, William Lubell<sup>6</sup>, José Carlos Rivera<sup>2,3</sup> and Sylvain Chemtob<sup>1,2,3\*</sup> 

## Abstract

**Background:** Inflammation and particularly interleukin-1 $\beta$  (IL-1 $\beta$ ), a pro-inflammatory cytokine highly secreted by activated immune cells during early AMD pathological events, contribute significantly to retinal neurodegeneration. Here, we identify specific cell types that generate IL-1 $\beta$  and harbor the IL-1 receptor (IL-1R) and pharmacologically validate IL-1 $\beta$ 's contribution to neuro-retinal degeneration using the IL-1R allosteric modulator composed of the amino acid sequence rytvela (as well as the orthosteric antagonist, Kineret) in a model of blue light-induced retinal degeneration.

**Methods:** Mice were exposed to blue light for 6 h and sacrificed 3 days later. Mice were intraperitoneally injected with rytvela, Kineret, or vehicle twice daily for 3 days. The inflammatory markers F4/80, NLRP3, caspase-1, and IL-1 $\beta$  were assessed in the retinas. Single-cell RNA sequencing was used to determine the cell-specific expression patterns of retinal *Il1b* and *Il1r1*. Macrophage-induced photoreceptor death was assessed ex vivo using retinal explants co-cultured with LPS-activated bone marrow-derived macrophages. Photoreceptor cell death was evaluated by the TUNEL assay. Retinal function was assessed by flash electroretinography.

(Continued on next page)

\* Correspondence: [sylvain.chemtob@umontreal.ca](mailto:sylvain.chemtob@umontreal.ca)

<sup>1</sup>Department of Pharmacology and Therapeutics, McGill University, Montreal, QC, Canada

<sup>2</sup>Departments of Pediatrics, Ophthalmology, and Pharmacology, Hôpital Maisonneuve-Rosemont Research Center, 5415 Boul L'Assomption, Montreal, QC H1T 2M4, Canada

Full list of author information is available at the end of the article



© The Author(s). 2020 **Open Access** This article is licensed under a Creative Commons Attribution 4.0 International License, which permits use, sharing, adaptation, distribution and reproduction in any medium or format, as long as you give appropriate credit to the original author(s) and the source, provide a link to the Creative Commons licence, and indicate if changes were made. The images or other third party material in this article are included in the article's Creative Commons licence, unless indicated otherwise in a credit line to the material. If material is not included in the article's Creative Commons licence and your intended use is not permitted by statutory regulation or exceeds the permitted use, you will need to obtain permission directly from the copyright holder. To view a copy of this licence, visit <http://creativecommons.org/licenses/by/4.0/>. The Creative Commons Public Domain Dedication waiver (<http://creativecommons.org/publicdomain/zero/1.0/>) applies to the data made available in this article, unless otherwise stated in a credit line to the data.

(Continued from previous page)

**Results:** Blue light markedly increased the mononuclear phagocyte recruitment and levels of inflammatory markers associated with photoreceptor death. Co-localization of NLRP3, caspase-1, and IL-1 $\beta$  with F4/80<sup>+</sup> mononuclear phagocytes was clearly detected in the subretinal space, suggesting that these inflammatory cells are the main source of IL-1 $\beta$ . Single-cell RNA sequencing confirmed the immune-specific expression of *Il1b* and notably perivascular macrophages in light-challenged mice, while *Il1r1* expression was found primarily in astrocytes, bipolar, and vascular cells. Retinal explants co-cultured with LPS/ATP-activated bone marrow-derived macrophages displayed a high number of TUNEL-positive photoreceptors, which was abrogated by rytvela treatment. IL-1R antagonism significantly mitigated the inflammatory response triggered in vivo by blue light exposure, and rytvela was superior to Kineret in preserving photoreceptor density and retinal function.

**Conclusion:** These findings substantiate the importance of IL-1 $\beta$  in neuro-retinal degeneration and revealed specific sources of *Il1b* from perivascular MPs, with its receptor *Il1r1* being separately expressed on surrounding neuro-vascular and astroglial cells. They also validate the efficacy of rytvela-induced IL-1R modulation in suppressing detrimental inflammatory responses and preserving photoreceptor density and function in these conditions, reinforcing the rationale for clinical translation.

**Keywords:** Retinal degeneration, Photoreceptors, cell death, Inflammation, Inflammasome, Interleukin-1, Interleukin-1 receptor, Rytvela

## Introduction

Photoreceptor cell death is a hallmark of many retinal degenerative disorders including age-related macular degeneration (AMD) [1–4], the leading cause of vision loss in the aging populations of developed countries [5]. Two types of AMD are clinically recognized: wet AMD, distinguished by choroidal neovascularization, and dry AMD, characterized by the degeneration of the retinal pigmented epithelium (RPE) and photoreceptors. Wet AMD is generally treated with anti-vascular endothelial growth factor therapies [6], while no therapy is currently available for dry AMD.

Substantial evidence points to inflammation as a key player in photoreceptor cell loss in retinal degenerative disorders including dry AMD [4, 7–13]. Accumulation of mononuclear phagocytes (MPs), a family of cells which includes monocytes, macrophages, and microglia, has been associated with photoreceptor damage in retinal degeneration [12, 14–18]. Under normal physiological conditions, the subretinal space and photoreceptor layer are devoid of MPs. Conversely, in pathological conditions, MPs are activated, invade the outer and subretinal space, and secrete pro-inflammatory cytokines, including tumor necrosis factor- $\alpha$ , interleukin (IL)-6, and, importantly, IL-1 $\beta$ , which is considered to play a major role in retinal degeneration [11, 19].

High levels of IL-1 $\beta$  are detected in the eyes of AMD patients [20] and the same applies to models of macular degeneration wherein IL-1 $\beta$  is generated by microglia/macrophages [21–23]. The NOD-like receptor family pyrin domain-containing 3 (NLRP3) inflammasome is the major mediator of IL-1 $\beta$  production in the retina [24, 25] and is required to activate caspase-1 which

catalyzes the processing of pro-IL-1 $\beta$  into active IL-1 $\beta$  [26, 27]. IL-1, in turn, primes the assembly of NLRP3 and further augments inflammatory cytokine production via positive feedback [28]. Previous studies have shown that some components of drusen and the C1q complement protein can activate the NLRP3 inflammasome in macrophages [25] and promote the secretion of IL-1 $\beta$  [29]; the same applies with lipofuscin when it accumulates with age [30]. Once activated, the IL-1 $\beta$  signal amplifies inflammation in rodent eyes by inducing expression of Chemokine (C-C motif) ligand 2 (*Ccl2*), Chemokine (C-X-C motif) ligand 1 (*Cxcl1*), and C-X-C motif chemokine ligand 10 (*Cxcl10*), which recruit leukocytes [21]. Concordantly, transcriptomic analysis of human retinas afflicted with AMD reveals upregulation of the same chemokines [31].

However, opposing observations on the role of IL-1 $\beta$  in retinal degeneration have been reported. For instance, pronounced sub-retinal inflammation and photoreceptor degeneration are observed in pigmented *Cx3cr1*-null mice subjected to light exposure; under these conditions, IL-1 receptor antagonist (IL-1Ra) is protective against photoreceptor cytotoxicity [32]. Similar conclusions have been drawn regarding the role of IL-1 $\beta$  in photo-oxidative damage to photoreceptors in rats [21]. Concordantly, IL-1 $\beta$  can induce apoptosis of retinal endothelium [33], neuronal precursor cells [34], and photoreceptors, but the precise mechanism of photoreceptor death in retinal degeneration remains unclear [22, 23, 32, 35]. On the other hand, LaVail [36] demonstrated protective effects of IL-1 $\beta$  on photoreceptors, while others failed to observe preservation of photoreceptors by IL-1Ra in light-exposed rodents [37]. Hence, collectively, the role of IL-1 $\beta$  in photoreceptor

degeneration is unclear and suggests possible opposing effects of IL-1 $\beta$  based on concentrations which can depend on cell types and presumed locations relative to targeted photoreceptors, as well as by genetic determinants including those that apply to the diverse signaling of the IL-1 receptor (IL-1R) resulting in neurodegeneration. Correspondingly, the specific identity of cells producing IL-1 $\beta$  and harboring the IL-1 receptor has not been clearly defined.

IL-1 $\beta$  can bind to two types of receptors, IL-1 receptor I (IL-1RI) and IL-1 receptor II (IL-1RII). The binding of IL-1 to IL-1R1 induces a conformational change that allows the binding of the IL-1 receptor accessory protein (IL-1RacP) to IL-1R1, which then triggers the inflammatory cascade [38]. IL-1RII acts as a decoy receptor as it binds IL-1 but does not transduce IL-1 signaling [39]. There are a limited number of anti-inflammatory therapies that target IL-1 signaling; this includes anakinra (commercially known as Kineret), a recombinant form of IL-1Ra that binds competitively to IL-1R and non-selectively blocks downstream signaling [40]. We had previously developed a novel all-D peptide allosteric modulator with the amino acid sequence rytvela, which is an intramolecular peptide derived from the sequence of IL-1RacP [41]. Intramolecular peptides function on the basis of disrupting protein-protein interactions [42], such as the interaction between IL-1R and IL-1RacP in the case of rytvela (remote from the IL-1 $\beta$  binding site), and may confer benefits such as functional selectivity, which is associated with improved efficacy and reduced side effects [43].

In the present study, we pharmacologically validate the role of IL-1 $\beta$  in a light-induced model of subretinal inflammatory photoreceptor degeneration [12, 18]. We hereby clarify using single-cell RNA sequencing-specific sources of IL-1 $\beta$  from perivascular MPs, and IL-1RI expression primarily on astroglia and vascular cells. We also show that rytvela (as well as the molecularly and pharmacologically distinct Kineret) inhibits inflammation and preserves photoreceptor density and function to a greater extent than Kineret in this model.

## Materials and Methods

### Animals

All animal experiments were approved by the Maison-neuve Rosemont Hospital Animal Care Committee and were performed in accordance with the Association for Research in Vision and Ophthalmology Statement for the Use of Animals in Ophthalmic and Visual Research. Male CD-1 mice (Charles River Laboratories, Kingston, NY) of 12–16 weeks of age were used in this study. We favored using these outbred mice since inbred mice may not reflect genetic diversity as observed in the human population. In addition, genetic background does not

appear to contribute significantly to the variation observed in measurements of phenotype [44]. Moreover, CD-1 mice are less susceptible to spontaneous lesions affecting the eye, which makes them a good model for pharmacological and long-term safety studies for ocular phenotypes [45]. CD-1 mice were housed with a 12-h light/dark cycle (100–200 lux) with water and normal diet food available ad libitum.

### IL-1 receptor antagonists

Kineret (Sobi, Biovitrum Stockholm, Sweden) was supplied as a 150 mg/mL solution and diluted to the required concentrations for all experiments with phosphate-buffered saline (PBS). Rytvela (Elim Biopharmaceuticals, Hayward, CA) was supplied as a lyophilized powder, dissolved in PBS, and diluted to the concentrations required for the experiments described below.

### Blue light exposure model

Mice were dark-adapted overnight, then pupils were dilated using topical atropine (Alcon) prior to light exposure. Mice were exposed to blue light from a light-emitting diode (wavelength 450 nm, Apluschoice) at a light intensity of 6,000 lux for 6 h and then returned to regular conditions under a standard 12-h light/dark cycle until sacrifice on day 3 post-illumination. Mice were intraperitoneally injected with IL-1 receptor antagonists Kineret (4 mg/kg/12 h) or rytvela (1.5 mg/kg/12 h), or with phosphate-buffered saline (PBS) twice a day starting on the day of illumination until day 3. These doses were determined from our previous study [33]. Subsequently, the mice were euthanized on day 3 by cervical dislocation under isoflurane anesthesia, and eyes collected.

### Retinal section preparation

Eyes were enucleated and fixed in 4% paraformaldehyde (PFA) for 1 h at room temperature and then rinsed twice with PBS. The cornea and lens were gently removed from the eye. Posterior eyecups were kept in 30% sucrose overnight and then frozen in optimal cutting temperature (OCT) medium. Sections of the entire retina along the optic nerve were cut into 10- $\mu$ m sagittal sections. Retinal sections were treated at room temperature for 1 h with a blocking solution consisting of 10% fetal bovine serum, 0.1% Triton X-100, and 0.05% Tween-20 in PBS. Retinal sections were then incubated overnight with primary antibodies, 1:200 fluorescein-labeled peanut agglutinin (PNA) (FL-1071) or 1:100 *Griffonia simplicifolia* Lectin I (GSL I) isolectin B4, Fluorescein (FL-1201) at 4 °C. The antibodies used were 1:100 NLRP3 (Abcam, ab91413), 1:100 IL-1 $\beta$  (Abcam, ab9722), 1:100 caspase-1 (BioVision, 3019), glial fibrillary acidic protein (GFAP) (Dako, Z0334), and

IL1R1 (Santa Cruz, sc-393998). The retinal sections were then washed thrice with PBS and incubated with a secondary antibody solution consisting of 1% bovine serum albumin (BSA), 0.1% Triton X-100, 0.05% Tween-20, 1:500 Alexa Fluor donkey 594 anti-rat (A21209, Invitrogen), and 1:500 Alexa Fluor 488 goat anti-rabbit (A11070, Invitrogen) for 2 h at room temperature. Retinal sections were washed thrice with PBS and then flat-mounted onto glass slides with coverslips and Fluoro-Gel mounting medium (Electron Microscopy Sciences, Hatfield, PA). Sections were imaged using a laser scanning confocal microscope (Olympus IX81 with Fluoview FV1000 Scanhead) with the Fluoview Software at 30X magnification. The integrated density of GFAP was determined using ImageJ (National Institutes of Health, Bethesda, MD, USA). The integrated density is the area above the threshold for the mean density minus the background.

#### Measurement of photoreceptor layer thickness

Fourteen measurements per central retinal section (with optic nerve) were performed at defined distances from the optic nerve. Analysis of outer nuclear layer thickness was performed using ImageJ. The area under the curve was integrated using Prism version 7.0A (GraphPad software).

The length of the photoreceptor cone segments was measured using ImageJ, with 4 to 6 measurements made per central retinal section.

#### Retinal flat mount preparation

Eyes were enucleated and fixed in 4% PFA for 1 h and then rinsed twice with PBS. The neuroretina was carefully separated from the RPE/choroid/sclera complex and processed for immunostaining. Retinas were treated at room temperature for 1 h with a blocking solution consisting of 1% BSA, 1% normal goat serum, 0.1% Triton X-100, and 0.05% Tween-20 in PBS. The retinas were then labeled overnight at 4 °C with gentle shaking using the following primary antibodies: 1:400 anti-F4/80 (ab6640, Abcam) and 1:500 anti-IL-1 $\beta$  (ab9722, Abcam). The retinas were then washed thrice with PBS and incubated with a secondary antibody solution consisting of 1% BSA, 0.1% Triton X-100, 0.05% Tween-20, 1:500 Alexa Fluor donkey 594 anti-rat (A21209, Invitrogen),

and 1:500 Alexa Fluor 488 goat anti-rabbit (A11070, Invitrogen) for 2 h at room temperature. Retinas were washed thrice with PBS and then flat-mounted onto glass slides with coverslips and Fluoro-Gel mounting medium (Electron Microscopy Sciences, Hatfield, PA). For MP quantification, images were captured and stitched together using the MosaiX feature of Axiovision 4.

#### Quantification of activated MPs in the subretinal space

F4/80-stained cells were counted on flat mounts with photoreceptor segments facing the objective. Cell numbers were expressed as the mean number of F4/80<sup>+</sup> cells per mm<sup>2</sup>.

#### Single-cell RNA sequencing analysis

The *Mus musculus* wild-type retina single-cell RNA sequencing datasets were obtained using the accession numbers GSM3854512, GSM3854514, GSM3854516, and GSM3854518 and analyzed using the Seurat R package [46]. Cells having a unique feature count between 100 and 4000, a total molecule number of less than 10000, and a mitochondrial RNA percentage of less than 25 were included. A global scaling normalization method, LogNormalize, was employed. This function normalizes the feature expression measurements for each cell by the total expression, multiplies this by a scale factor (10,000 by default), and log-transforms the result. After normalization, the scale expression (z-scores for each gene) was calculated for downstream dimensional reduction. After integration using the Seurat alignment procedures, the integrated matrix was then used for downstream analysis and visualization. Principal component analysis was run on the scaled integrated data and the results of dimensionality reduction were visualized with Uniform Manifold Approximation and Projection (UMAP). The clusters obtained were annotated using the markers provided by Heng et al. [47]. The expression of the genes *Il1r1* and *Il1b* were illustrated using dot plots.

The *Mus musculus* immune single-cell RNA sequencing datasets were obtained using the accession number GSE126783 and analyzed using the Seurat R package [46]. Light-damaged and control Cx3cr1<sup>YFP+</sup> cells were filtered based on unique feature counts and mitochondrial counts. Cells having a unique feature count of less

**Table 1** List of primers used for qPCR experiments

Gene	Forward primer	Reverse primer
<i>Il1b</i>	5'-CTGGTACATCAGCACCTCACA-3'	5'-GAGCTCCTTAACATGCCTG-3'
<i>Il6</i>	5'-ACAGAAGGAGTGGCTAAGGA-3'	5'-AGGCATAACGCACTAGGTTT-3'
<i>Ccl2</i>	5'-CCACAACCACCTCAAGCACT-3'	5'-AGGCATCACAGTCCGAGTCA-3'
<i>Actb</i>	5'-GTGGGCCGCACAAGGCACCAA-3'	5'-CTCTTTGATGTCACGCACGA-3'
<i>18S</i>	5'-CCTGCGGCTTAATTTGACTCA-3'	5'-AGCTATCAATCTGTCAATCTGTGTC-3'

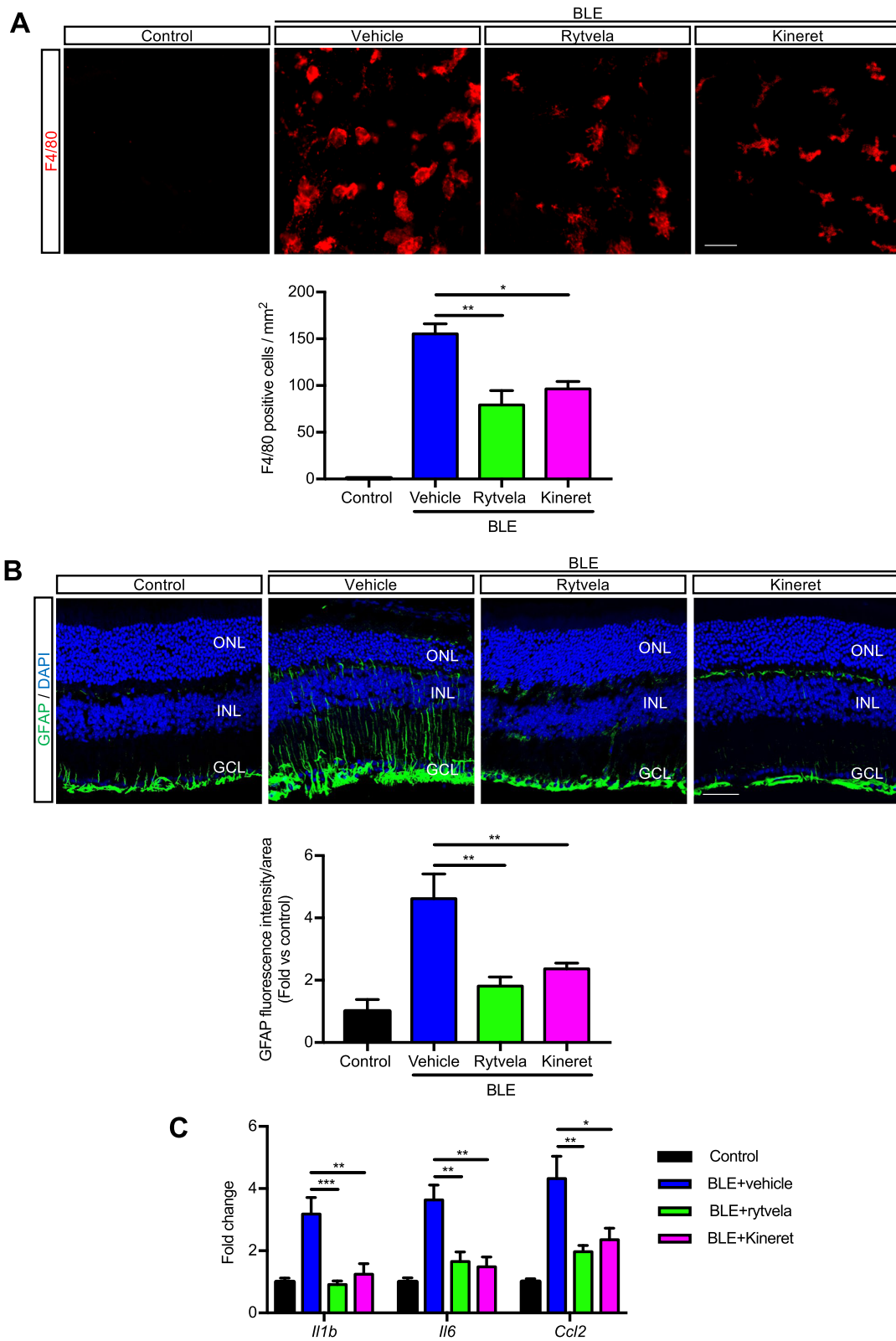


**Fig. 1** (See legend on next page.)

(See figure on previous page.)

**Fig. 1** Subretinal macrophage infiltration and gliosis in blue light exposure to mice. **a** Representative images of retinal flat mounts showing infiltration of F4/80-labeled mononuclear phagocytes (red) of mice exposed or not to blue light exposure (BLE) and treated with vehicle, rytvela, or Kineret. Scale bar 50  $\mu$ m. The graph represents compiled data on F4/80<sup>+</sup> cell density in the subretina presented as a histogram. Data are expressed as mean  $\pm$  SEM and analyzed by one-way ANOVA with Holm-Sidak correction for multiple comparisons;  $n = 4-8$  per group.  $^{**}p < 0.01$ ,  $^{*}p < 0.05$ . **b** Representative images of GFAP immunoreactivity (green) showing retinal gliosis in blue light-exposed animals treated with vehicle, and suppressed by rytvela and Kineret. Sections were co-stained with DAPI (blue) to show cell nuclei. Scale bar 50  $\mu$ m. ONL: outer nuclear layer; INL: inner nuclear layer; GCL: retinal ganglion cell layer. The graph represents the quantitative analysis of GFAP immunofluorescence intensity compared with control light unexposed values set at mean of 1. Data are expressed as mean  $\pm$  SEM and analyzed by one-way ANOVA with Holm-Sidak correction for multiple comparisons for  $n = 3-6$  per group.  $^{**}p < 0.01$  (C) mRNA expression of *Il1b*, *Il6*, and *Ccl2*, standardized to control light unexposed values set at mean of 1. Data are expressed as mean  $\pm$  SEM and analyzed by one-way ANOVA with Holm-Sidak correction for multiple comparisons for  $n = 3-6$  per group.  $^{***}p < 0.001$ ,  $^{**}p < 0.01$ ,  $^{*}p < 0.05$

than 4000 and a mitochondrial RNA percentage of less than 10 were kept. The 2 Seurat Objects were then merged. An integration was performed on this object following the Integration and Label Transfer Vignette (SATIJA LAB). The integrated matrix was then used for downstream analysis and visualization. Principal component analysis was run on the scaled integrated data and the results were visualized with UMAP. The clusters obtained were annotated using the markers provided by O’Koren et al. [48]. All the microglia sub-clusters were regrouped together, and 3 different cell types were annotated: microglia, perivascular macrophages (pv MFs), and monocyte-derived macrophages (mo MFs). The expression of the genes *Il1r1* and *Il1b* were illustrated using dot plots.

#### Terminal deoxynucleotidyl transferase dUTP nick end labeling assay

TUNEL staining was performed according to the manufacturer’s protocol (In Situ Cell Death Detection Kit; Roche Diagnostics). Briefly, retinal flat mount or retinal sections were fixed in 4% PFA for 30 min and washed in PBS. Flat mounts or sections were then incubated for 90 min at 37 °C with the reaction mixture and the reaction was stopped by washing with PBS. Nuclei were stained with 4’, 6-diamidino-2-phenylindole (DAPI, Sigma, St. Louis, MO, USA). Images were captured with a laser scanning confocal microscope (Olympus IX81 with Fluoview FV1000 Scanhead) with the Fluoview Software at 30X magnification.

#### Isolation of bone marrow-derived monocytes

Bone marrow-derived monocytes (BMDMs) were harvested from 12- to 16-week-old CD-1 mice sacrificed by cervical dislocation. Total mononuclear cells were flushed from femurs and tibiae with PBS. to subsequently isolate the BMDM population. Briefly, the suspension was centrifuged at 1500 rpm for 10 min. The supernatant was discarded, and the pellet was resuspended in Dulbecco’s Modified Eagle Medium (DMEM) supplemented with 10% FBS (085-150, Wisent Bioproducts), 1% penicillin and streptomycin, and 0.125  $\mu$ g/mL

macrophage colony-stimulating factor (M-CSF) (576406; Biolegend). The suspension of BMDMs was filtered using sterile cell strainers (40  $\mu$ m; 352340; Corning) and seeded in 24-well plates. The culture medium was renewed every 2 days for 1 week.

#### BMDM and retinal explant incubation

BMDMs were treated or not with 50 ng/mL lipopolysaccharide (LPS) (*Escherichia coli* 10004557; Thermo Fisher) for 24 h and then 1 mM of adenosine triphosphate (ATP; R0441; Thermo Fisher Scientific) was added for 30 min. BMDMs were washed twice with DMEM supplemented with 0.2% BSA (800-095-EG; Wisent). BMDMs were cultured for 24 h and the supernatant served as conditioned media. Mouse retinas were prepared and placed on either 100,000 adherent BMDMs for 18 h at 37 °C in DMEM with 0.2% BSA or in BMDM-derived conditioned media in the absence or presence of rytvela (1  $\mu$ M), Kineret (1.5 mg/mL), or an anti-IL-1 $\beta$  antibody (150 ng/mL, Abcam 9722). Doses of rytvela and Kineret were determined based on our previous study [49]. After 18 h, the explants were evaluated by TUNEL assay.

#### Quantitative RT-PCR

Total RNA was extracted from mice retinas using the RNeasy mini kit (Qiagen) according to the manufacturer’s protocol and was reverse transcribed using iScript™ Reverse Transcription Supermix (Bio-Rad) according to the manufacturer’s guidelines to generate cDNA. qPCR reactions were performed using 25 ng of sample cDNA, 2  $\mu$ M of specific primers for the selected mRNAs (Table 1), and Universal SYBR Green Master Mix (BioRad). Relative expression (RQ =  $2^{-\Delta\Delta CT}$ ) was calculated using a detection system (ABI Prism 7500, Applied Biosystems, Foster City, CA, USA) and normalized to  $\beta$ -actin (*Actb*) and 18S.

#### Western blotting

Proteins were extracted from mice retinas by sonication in lysis buffer RIPA buffer (pH = 8) containing 50 mM Tris-HCl, 150 mM NaCl, 5 mM EDTA, 1% Triton 100 $\times$ , 0.5% sodium deoxycholate, 0.1% SDS, and a cocktail of

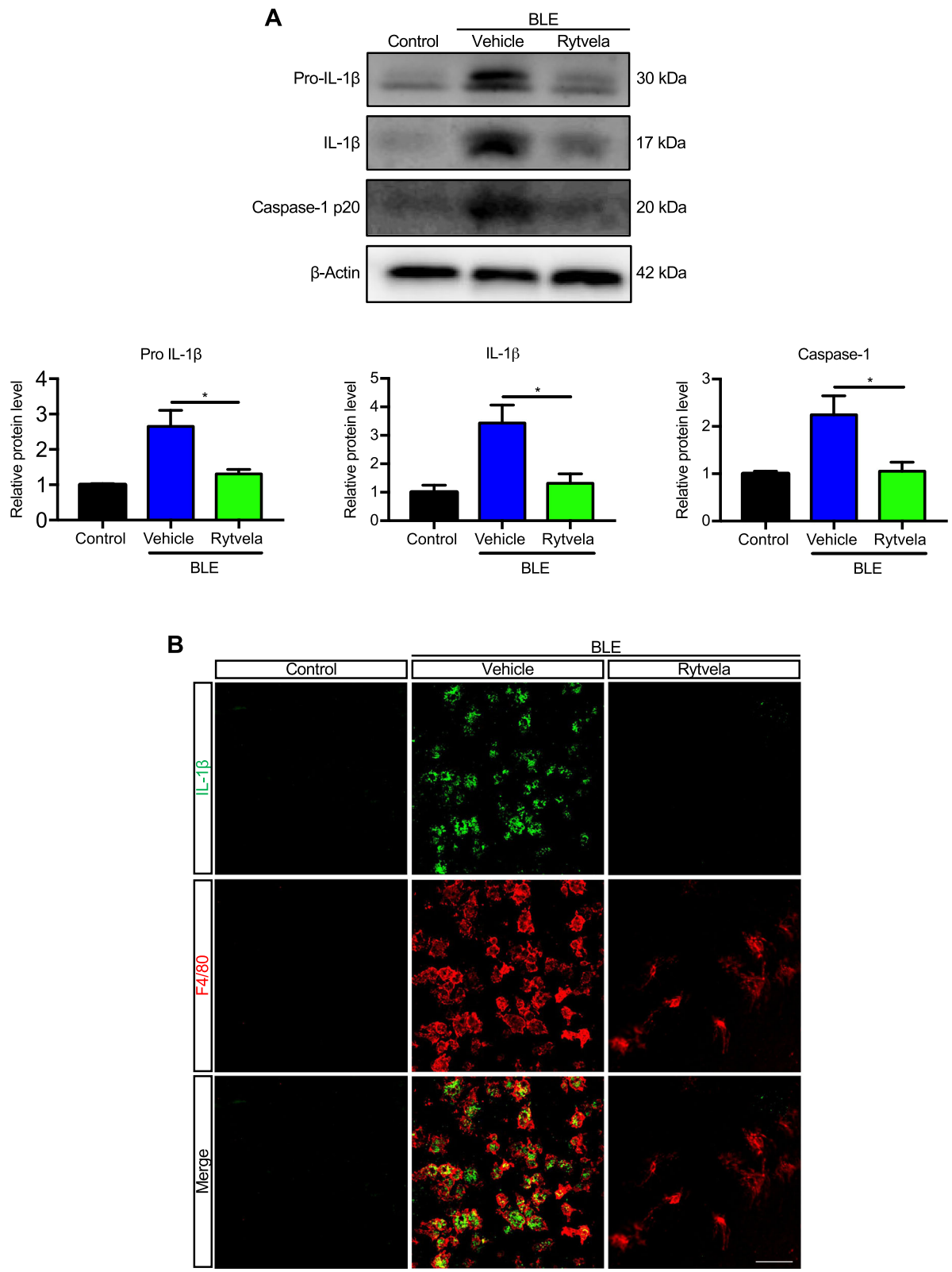


**Fig. 2** (See legend on next page.)

(See figure on previous page.)

**Fig. 2** IL-1 $\beta$  production in blue-light-exposed mice. **a** Representative western blots (top panel) showing the expression of uncleaved pro-IL-1 $\beta$ , mature IL-1 $\beta$ , and cleaved caspase-1 p20 in retinal samples from blue light-exposed animals untreated (vehicle) or treated with rytvela and compared with non-illuminated animals (control). The bottom panel depicts compiled data in histogram format. Data are expressed as mean  $\pm$  SEM and analyzed by independent *t* tests; *n* = 3–6 per group. \*\**p* < 0.01, \**p* < 0.05. **b** Representative images of retinal flat mounts showing co-localization of IL-1 $\beta$  (green) in mononuclear phagocytes F4/80<sup>+</sup> cells (red) from blue light-exposed animals treated with vehicle or rytvela. Mice exposed to blue light and treated with rytvela displayed less IL-1 $\beta$  immunoreactivity; retinal samples from non-illuminated animals showed no positive reaction. *n* = 6 per group. Scale bar 50  $\mu$ m

protease and phosphatase inhibitors (MiniComplete, PhosphoStop, and PMSF, Roche, Bâle, Switzerland). Protein concentrations were determined using the Bicinchoninic Acid Protein Assay Kit (Pierce, Rockford, IL, USA). Thirty micrograms of protein per sample were electrophoresed on 15% sodium dodecyl sulfate-polyacrylamide gels using an electrophoresis system (Mini-Protean Tetra System, Bio-Rad, Hercules, CA, USA) and then transferred onto polyvinylidene difluoride membranes (Millipore, Billerica, MA, USA). Membranes were blocked with 5% skim milk in Tris-buffered saline containing 0.1% Tween-20 for 1 h at room temperature, and incubated with the following primary antibodies: 1:800 IL-1 $\beta$  (Abcam, ab9722), 1:500 caspase-1 (BioVision, 3019), and 1:1000  $\beta$ -actin (Santa Cruz, sc47778) then incubated with 1:6000 horseradish peroxidase-conjugated secondary antibodies (Millipore, AP307P and Millipore, AP308P). Densitometric analysis of western blotting bands was quantified using the ImageJ software and normalized to  $\beta$ -actin.

#### Enzyme-linked immunosorbent assay

Conditioned media from BMDMs incubated with retinal explants were collected. The concentrations of IL-1 $\beta$  were measured using a commercial ELISA kit (R&D Systems, MLB00C) according to the manufacturer's instructions. Calibration curves were prepared using purified standards for IL-1 $\beta$  which were provided as part of the ELISA kit.

#### Electroretinogram

Electroretinograms (ERGs) were recorded using an Espion ERG Diagnosys apparatus equipped with a Color-Dome Ganzfeld stimulator (Diagnosys LLC, Lowell, MA). Mice were initially dark-adapted overnight and anesthetized intraperitoneally with a mix of ketamine (100 mg/kg) and xylazine (20 mg/kg). Corneas were anesthetized with proxymetacaine hydrochloride (0.5% Alcaine; Alcon, Fort Worth, TX, USA) and pupils dilated with 0.5% atropine (Alcon, Fort Worth, TX, USA). Body temperature was maintained at 37.5 °C with a heating pad. ERGs were measured using corneal DTL Plus electrodes (Diagnosys LLC), a forehead reference electrode, and a ground electrode subcutaneously in the tail. To evaluate rod photoreceptor function (scotopic ERG),

five-strobe flash stimuli were presented with flash intensities of 0.01 candela\*second/meter<sup>2</sup> (cds/m<sup>2</sup>), 0.1 cds/m<sup>2</sup>, 0.5 cds/m<sup>2</sup>, 1.0 cds/m<sup>2</sup>, and 3.0 cds/m<sup>2</sup>. Six waveforms were averaged per light intensity. All procedures were performed in a dark room under dim red-light illumination. The amplitude of the a-wave was measured from baseline to the primary negative peak, and b-wave was measured from the trough of the a-wave to the maximum of the fourth positive peak.

#### Statistical analysis

Values are presented as means  $\pm$  standard error of the mean (SEM). Data were analyzed by independent *t*-tests or one-way analysis of variance (ANOVA) followed by post hoc Holm-Sidak tests for comparison of means. Statistical significance was set at *p* < 0.05. Statistical analysis was performed using Prism 7.0A (GraphPad Software).

## Results

### Blue light induces subretinal macrophage infiltration, which is suppressed by IL-1R antagonism

Blue light elicited substantial infiltration of MPs as evidenced by the presence of F4/80<sup>+</sup> cells in the outer and subretina (Fig. 1a), consistent with reported observations [12, 18]. MPs are not seen in the subretinal space of unexposed (intact) retinas. Kineret, and to a slightly greater extent, rytvela mitigated this MP infiltration and maintained MP morphology in a ramified, quiescent state, rather than the activated amoeboid state seen in vehicle-treated animals (Fig. 1a). Glial fibrillary acidic protein (GFAP), a marker of retinal gliosis [50, 51] which is up-regulated upon MP activation [52] and used as an index of retinal degeneration, was dramatically increased throughout most of the entire retina (Fig. 1b); this effect was largely prevented by rytvela and Kineret. Concomitantly, light-induced increases in pro-inflammatory *Il1b*, *Il6*, and *Ccl2* mRNA levels were also significantly reduced by the IL-1R inhibitors rytvela and Kineret (Fig. 1c). Similar observations were made for inflammasome components and products, whereby increased blue light-induced NLRP3, caspase-1, and IL-1 $\beta$  at different stages of maturation (Fig. 2a) co-localized in F4/80<sup>+</sup> MPs (Figs. 2b and 3). Of relevance, retinal flat-mount staining revealed that IL-1 $\beta$  largely co-localized with



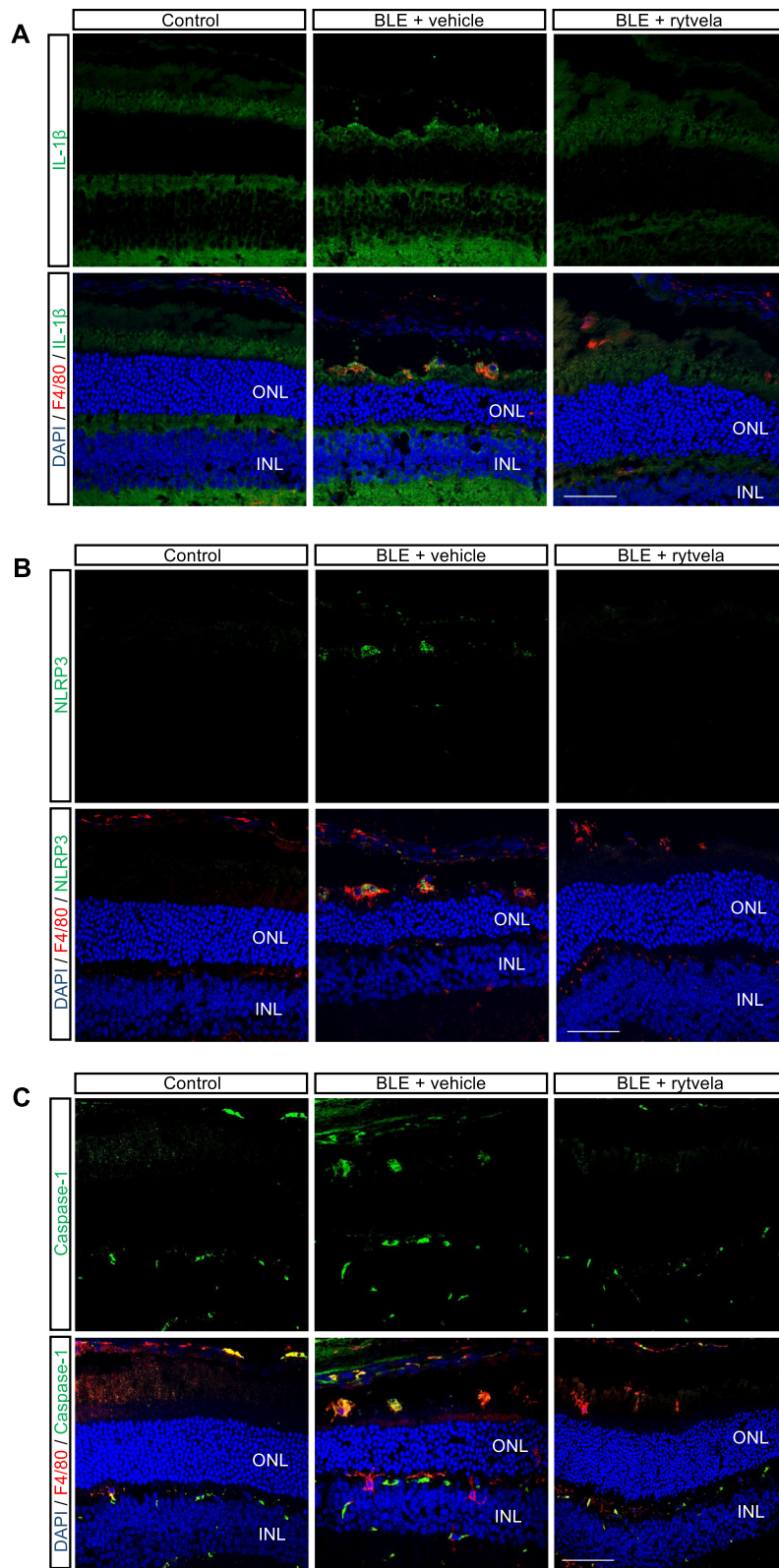


**Fig. 3** (See legend on next page.)

(See figure on previous page.)

**Fig. 3** Subretinal distribution of IL-1 $\beta$ , inflammasome (NLRP3), and caspase-1 after blue light exposure (BLE). Representative confocal images showing co-immunoreactivity of **a** IL-1 $\beta$  (green), **b** NLRP3 (green), and **c** caspase-1 (green) with MPs F4/80<sup>+</sup> cells (red) in the subretinal space of animals non-exposed (Control) and exposed to blue light (BLE) treated or not with rytvela. Cell nuclei were counterstained with DAPI (blue). Rytvela reduced immunoreactivity of IL-1 $\beta$ , NLRP3, and caspase-1.  $n = 4-5$  per group. Scale bar 50  $\mu$ m. ONL: outer nuclear layer; INL: inner nuclear layer

MPs (Fig. 2b), suggesting that infiltrating MPs are the major source of this pro-inflammatory cytokine.

### Single-cell RNA-seq analysis of *Il1b* and *Il1r1* expression in the retina

We analyzed the transcriptomic profiles of *Il1b* and its receptor *Il1r1* in the mouse retina. Single-cell mRNA transcriptomic analysis using 10 $\times$  Genomics revealed that immune cells are the main producers of *Il1b* in the retina and that *Il1r1* is mostly expressed in vascular cells (pericyte and endothelial cells) as well as astrocytes and bipolar cells (Fig. 4a). More importantly, *Il1r1* expression was not detected in photoreceptors and MPs (Fig. 4a). We next analyzed the proportions of different FACS-sorted live *Cx3cr1* MPs in control and light-damaged retinas. Among the 3 different cell types identified (Fig. 4b), light-damaged retinas showed a higher proportion of mo MF cells compared with the non-illuminated retinas (Fig. 4b, c), while microglia and pv MF distributions remained relatively unaffected. However, we found that *Il1b* was only upregulated in pv MFs but not in mo MFs or microglial cells in light-challenged mice compared with control (Fig. 4d). Expression of IL-1R1 was confirmed by immunofluorescence, showing that it colocalizes with GFAP and IB4 lectin in astrocytes and blood vessels, respectively (Fig. 4e, f), but not in MPs (Suppl Fig. 1).

### Suppression of subretinal inflammation preserves photoreceptor integrity

Next, we evaluated whether the suppression of subretinal inflammation using rytvela or Kineret was associated with preservation of photoreceptor integrity. Mice exposed to blue light experienced significant photoreceptor degeneration evidenced by a thinner outer nuclear layer (ONL; Fig. 5a), a loss of cone inner and outer segments (evaluated by peanut agglutinin [PNA] staining; Fig. 5b), high apoptotic rate in the ONL corroborated by augmented TUNEL positivity (Fig. 5c), and associated loss of the a-wave ERG amplitude generated from the photoreceptors (Fig. 6a). At an optimal flash intensity of 3.00 cds/m<sup>2</sup>, the a-wave amplitude of light-exposed animals decreased by half compared with the control group; as expected, b-wave amplitude was also lower in vehicle-treated animals since it is triggered in bipolar and Müller cells by the a-wave signal (Fig. 6b). Rytvela and Kineret prevented apoptosis (Fig. 5c, d) and preserved photoreceptor layer thickness, including its outer segments (Fig. 5a, b), and

photoreceptor function, with rytvela apparently being more effective than Kineret (Figs. 5a, b; and 6).

### Rytvela protects against macrophage-induced photoreceptor cell death in an ex vivo model

We next proceeded to clarify if inflammation triggered by inflammasome activators, notably LPS, causes photoreceptor cell death, and if inhibition of IL-1 $\beta$  would prevent the latter. To evaluate this mechanism, we induced a pro-inflammatory phenotype in isolated murine BMDMs stimulated with LPS/ATP (which also stimulates formation of mature IL-1 $\beta$  [53]; Fig. 7a). LPS/ATP-stimulated BMDMs were incubated facing the photoreceptor layer of neuroretinal explants in the presence or absence of the IL-1R antagonists rytvela (1  $\mu$ M) or Kineret (1.5 mg/mL) (Fig. 7a). Photoreceptor apoptosis was quantified by measuring TUNEL-positive cells in retinal explants. Exposure of retinal explants to LPS/ATP-stimulated BMDMs caused pronounced apoptosis of photoreceptors as witnessed by high numbers of TUNEL-positive cells (Fig. 7b); rytvela and Kineret prevented LPS/ATP-induced photoreceptor cell death. The number of TUNEL-positive cells did not differ between retinal explants cultured in the absence of BMDMs and the presence of non-activated BMDMs. In order to determine whether IL-1R inhibition in the neuroretina has a protective effect on photoreceptors, we treated neuroretinas with conditioned medium from BMDMs stimulated or not with LPS/ATP. Conditioned media from LPS/ATP-stimulated BMDMs caused an increase in the number of TUNEL-positive cells that was prevented by treating the neuroretina with rytvela or Kineret; these treatments did not affect the levels of IL-1 $\beta$  (Fig. 7c, d). To further clarify that IL-1 $\beta$  from activated BMDMs is involved, we used an IL-1 $\beta$ -neutralizing antibody which abrogated cell death (Fig. 7c). Taken together, these in vivo and ex vivo observations highlight the role of IL-1 $\beta$  and show that modulation of IL-1R signaling using rytvela (or IL-1R antagonist Kineret) interferes with detrimental subretinal inflammation in models of retinal phototoxicity and preserves photoreceptor density and function.

### Discussion

Neuroinflammation-induced photoreceptor cell death is a common feature of several ocular neurodegenerative disorders, including retinitis pigmentosa and AMD [54].

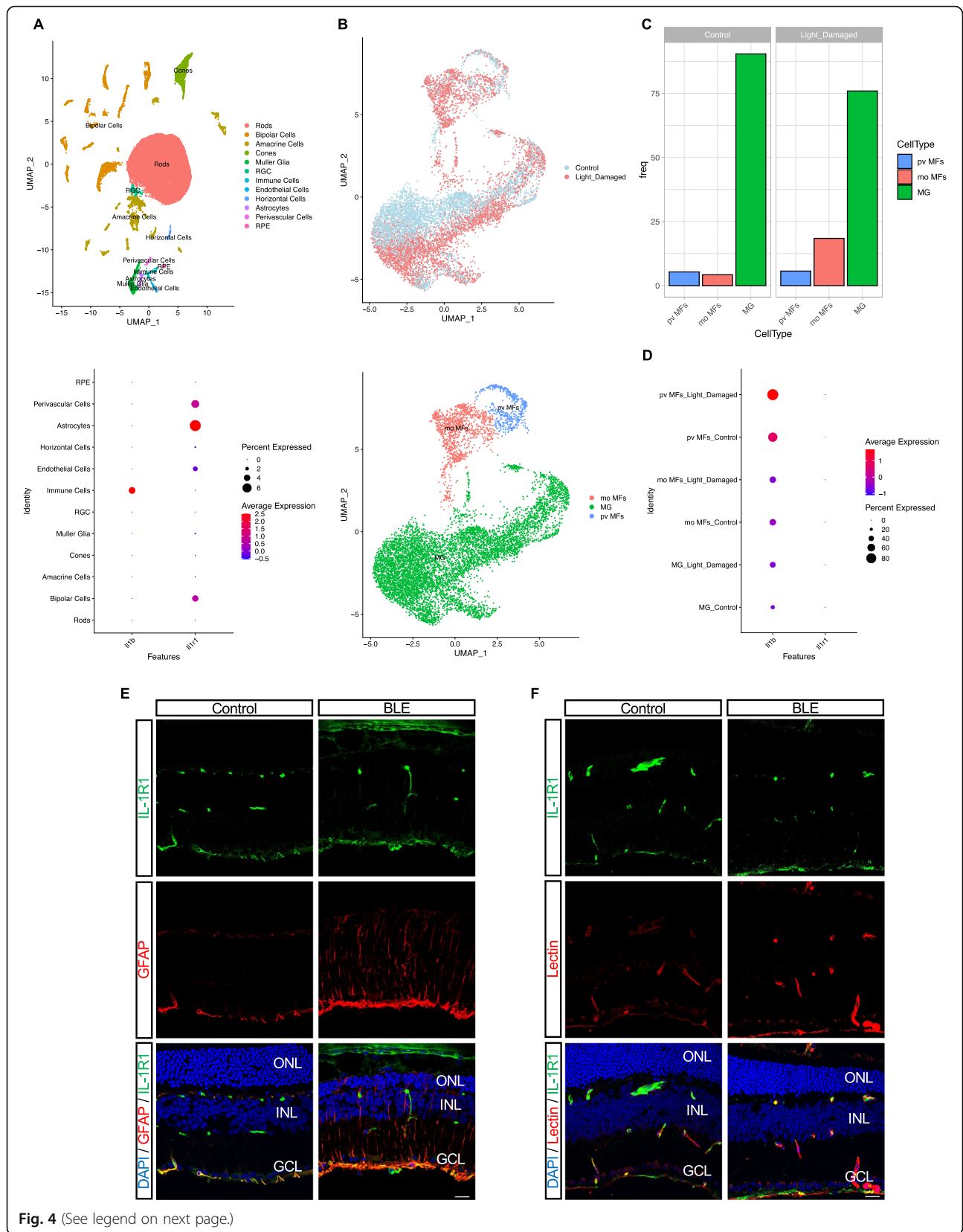


**Fig. 4** (See legend on next page.)

(See figure on previous page.)

**Fig. 4** Expression of *Il1b* and *Il1r* genes across retinal cell clusters. **a** UMAP plot of droplet-based single-cell RNA sequencing (scRNA-seq) data obtained using 10x Genomics technology and representing retinal cell type from adult mouse retina ( $n = 4$ , 10–16 weeks). The plot shows a two-dimensional representation of global gene expression relationship among 33942 cells clustered into 12 retinal cell types (top panel). The expression levels of *Il1r1* and *Il1b* are represented as dot plots across all the 12 cell types; larger dots indicate broader expression within the cluster; deeper red denotes a higher expression level (bottom panel). **b** UMAP plot of droplet-based scRNA-seq data obtained using 10x Genomics technology showing different clusters (top panel). UMAP plot of droplet-based single-cell RNA sequencing (scRNA-seq) data obtained using 10x Genomics technology and representing retinal cell types from control and light-damaged (LD) adult mouse retina. scRNA-seq data were generated on fluorescence-assisted cell sorting (FACS)-sorted live Cx3cr1<sup>YFP+</sup> cells from pooled neuroretinas of normal ( $n = 5$ ) and LD ( $n = 8$ ) mice. MG: microglia; pv MFs: perivascular macrophages; mo MFs: monocyte-derived macrophages. The plot shows a two-dimensional representation of global gene expression relationship among 10582 cells clustered into 3 retinal cell types (bottom panel). **c** Bar plot representation of Cx3cr1<sup>YFP+</sup> cell proportions in different conditions. **d** The expression levels of *Il1r1* and *Il1b* are represented as dot plots across all the 3 immune cell types; larger dots indicate broader expression within the cluster; deeper red denotes a higher expression level. Representative confocal images showing co-immunoreactivity of IL-1R1 (green) with **e** GFAP<sup>+</sup> cells (red) in the ganglion cell layer and **f** lectin (red).  $n = 4$  per group. Scale bar 20  $\mu$ m. ONL: outer nuclear layer; INL: inner nuclear layer; GCL: ganglion cell layer

The recruitment and activation of MPs are key components in the progressive loss of photoreceptors in these types of ocular disorders [55, 56]. Several studies have suggested that pro-inflammatory mediators released by these infiltrating immune cells in the subretinal space are the main contributors to neuronal damage [57–59]. In this context, the major proinflammatory cytokine IL-1 $\beta$  has been suggested to promote acute neuronal loss in experimental studies and has been implicated in chronic neurodegenerative disorders [60–63], including those of the eye [11]. IL-1 $\beta$  levels are found to be increased in the vitreous humor of patients with AMD [20] and have been reported to contribute to photoreceptor degeneration in different animal models [21, 23, 32]. Yet, experimentally, a cytotoxic role for IL-1 $\beta$  has been questioned by others [36, 37], inferring possible distinct mechanisms including those based on IL-1 $\beta$  concentration and/or genetic determinants including those applied to the diversity in IL-1RI-coupled signaling processes. Moreover, the identity (and presumed location) of cells generating IL-1 $\beta$  and harboring IL-1RI remains to be clarified in order to better elucidate the role that IL-1 $\beta$  plays in retinal degeneration.

The present study used a blue light-triggered model of inflammation-induced photoreceptor toxicity, which is commonly utilized [12] to experimentally recapitulate the phenotypic changes observed in neuro-retinal degenerative disorders [64, 65]. We observed infiltration/activation of MPs associated with increased pro-inflammatory cytokines, including IL-1 $\beta$  and photoreceptor cell death. Essentially, pv MFs were the main source of elevated *Il1b* expression, whereas the receptor *Il1r1* was separately expressed on astroglia and vascular cells. The detrimental effects of light-induced inflammation were prevented by treatment with a negative modulator of IL-1R, to an extent superior to that observed with an orthosteric antagonist.

Under physiological conditions, the subretinal space hardly harbors any MPs due to immunosuppression

mediated by inhibitory signals from neurons [66] and RPE cells [67]. However, MPs migrate to the subretinal space upon damage to the photoreceptors and/or RPE cells to scavenge cell debris in a process of efferocytosis which does not involve inflammatory responses [68]. With time upon exposure to light, exaggerated signals generated by trans-retinal Müller cells [55], RPE [69], and other MPs [56]. Activated MPs (revealed by their amoeboid morphology, absence of cell processes, and inflammatory cytokine profile) can contribute to retinal gliosis wherein Müller cells further release factors that amplify the inflammatory response [70]. In this sense, we showed augmented GFAP immunoreactivity in Müller glia associated with subretinal MP infiltration after blue light exposure. Although one of the roles of Müller cells is to protect tissues from damage, their over-activation can contribute to neurodegeneration and curtail regenerative processes [71]; concordantly, GFAP gene knockout prevents gliosis and protects photoreceptors [72]. Relevantly, the IL-1R modulator rytvela suppressed MP activation and recruitment, minimized gliosis, and exerted neuroprotection.

MPs are reported to elicit their pathogenic effects at least in part through IL-1 $\beta$  [32]. We detected infiltrating MPs as the main source of IL-1 $\beta$  associated with photoreceptor phototoxicity. In support of the fact that the NLRP3 inflammasome is a key regulator of IL-1 $\beta$  maturation via the activation of caspase-1 [73], we observed the colocalization of the inflammasome components NLRP3, caspase-1, and IL-1 $\beta$  in infiltrating subretinal MPs (F4/80<sup>+</sup>). Our findings reveal that IL-1R antagonism suppresses IL-1 $\beta$  production as well as neuroretinal phototoxicity in cells that separately express IL-1 $\beta$  and IL-1RI. Rytvela prevented elevations in IL-1 $\beta$  levels after blue-light exposure mostly by reducing the accumulation of IL-1 $\beta$ -producing MPs into the subretinal space. It was also shown to reduce activation of glial cells (gliosis), which is reported to upregulate IL-1 $\beta$  production via ATP release and activate the inflammasome in a P2X7-

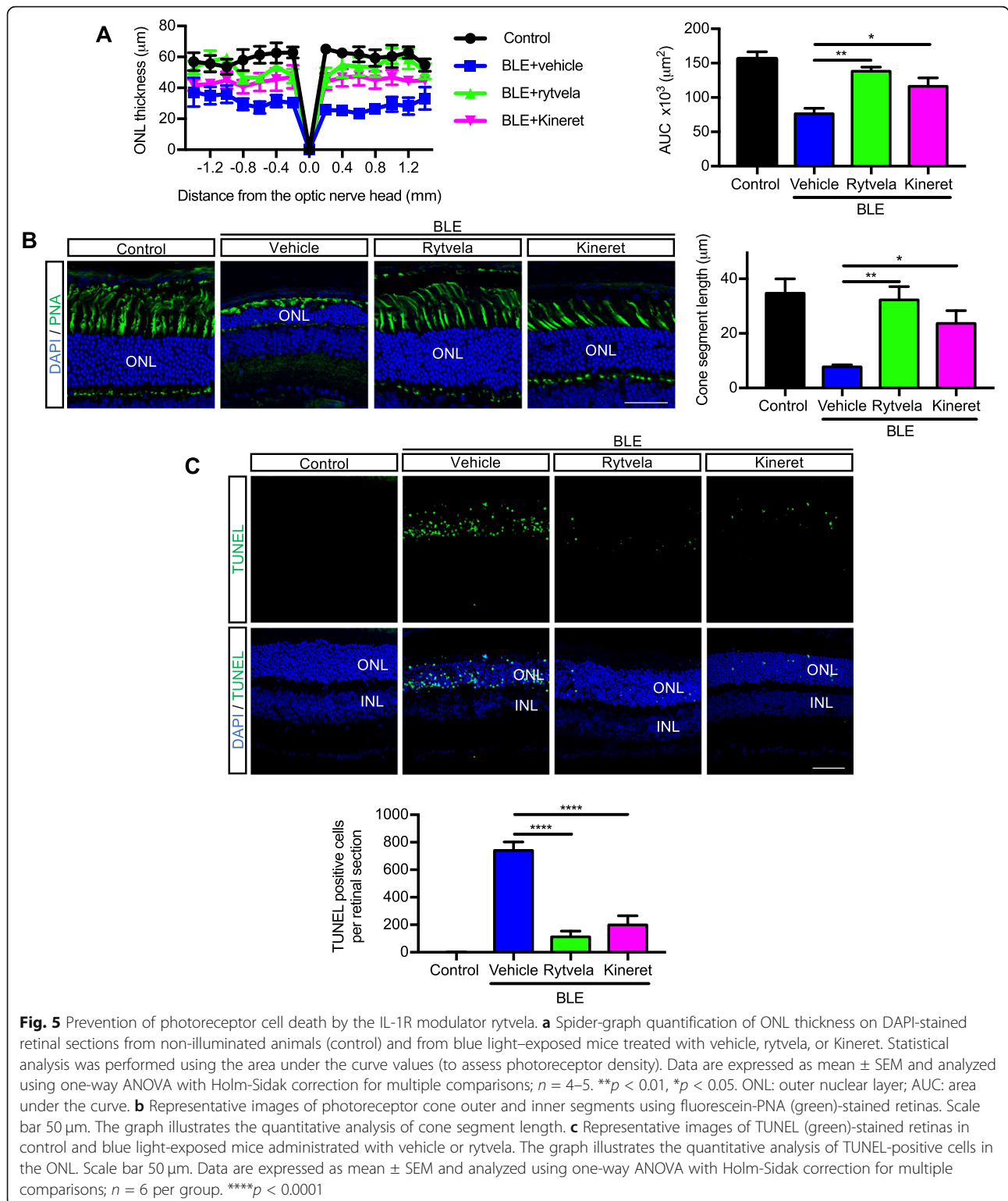
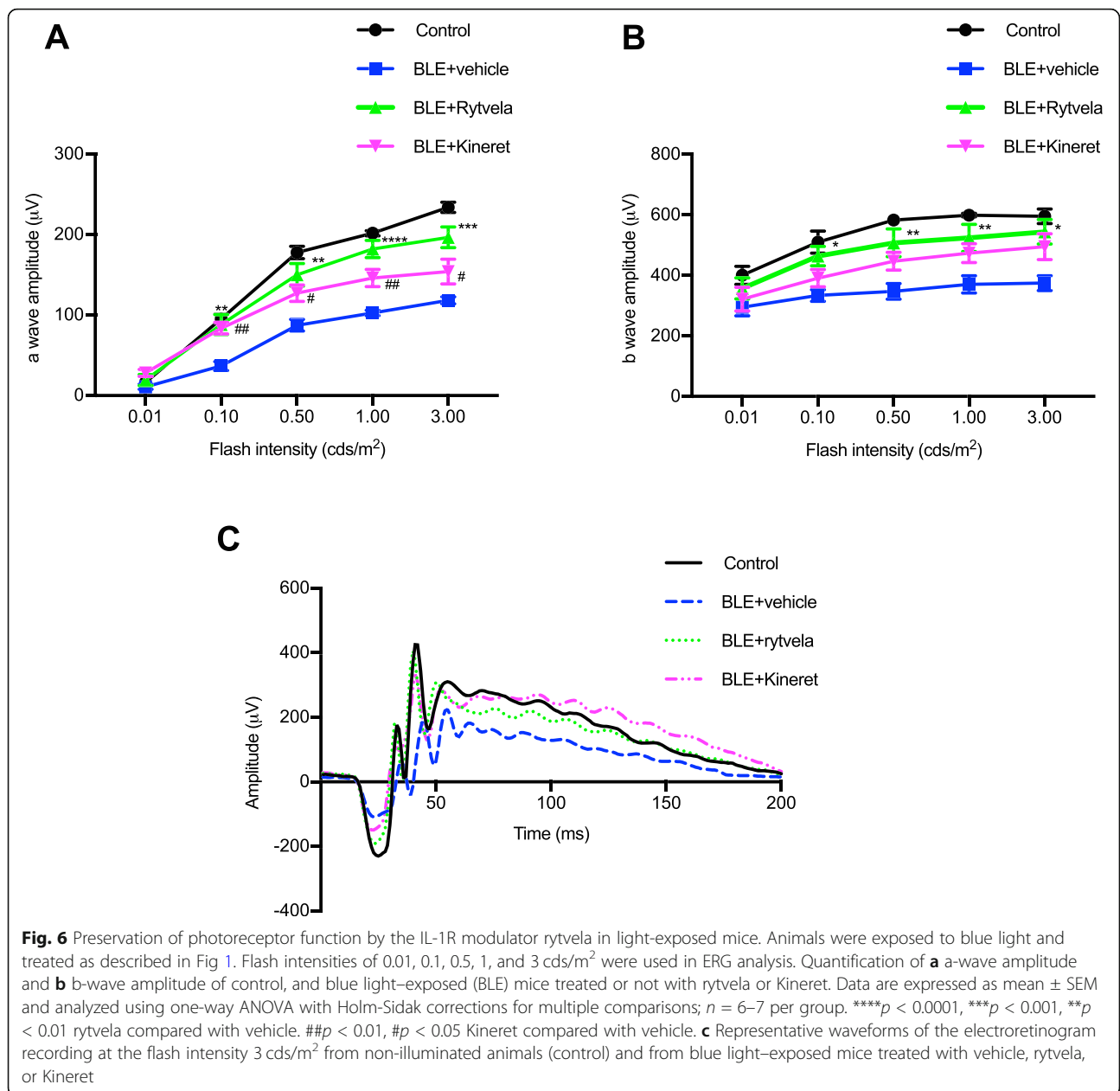


**Fig. 5** Prevention of photoreceptor cell death by the IL-1R modulator rytvela. **a** Spider-graph quantification of ONL thickness on DAPI-stained retinal sections from non-illuminated animals (control) and from blue light-exposed mice treated with vehicle, rytvela, or Kineret. Statistical analysis was performed using the area under the curve values (to assess photoreceptor density). Data are expressed as mean ± SEM and analyzed using one-way ANOVA with Holm-Sidak correction for multiple comparisons;  $n = 4-5$ .  $**p < 0.01$ ,  $*p < 0.05$ . ONL: outer nuclear layer; AUC: area under the curve. **b** Representative images of photoreceptor cone outer and inner segments using fluorescein-PNA (green)-stained retinas. Scale bar 50 μm. The graph illustrates the quantitative analysis of cone segment length. **c** Representative images of TUNEL (green)-stained retinas in control and blue light-exposed mice administrated with vehicle or rytvela. The graph illustrates the quantitative analysis of TUNEL-positive cells in the ONL. Scale bar 50 μm. Data are expressed as mean ± SEM and analyzed using one-way ANOVA with Holm-Sidak correction for multiple comparisons;  $n = 6$  per group.  $****p < 0.0001$

dependent mechanism [74]; cytotoxicity is also known to release ATP (and high mobility group box 1 [HMGB1]) to stimulate IL-1β release by macrophages. Rytvela (and Kineret) in turn suppresses IL-1RI-dependent

(photoreceptor) apoptotic processes involving mechanisms such as TRIF [75], IL-8 [76], glutamate transport [77], and reactive oxygen/nitrogen species [78]. Hence, one can envisage that light exposure triggers a

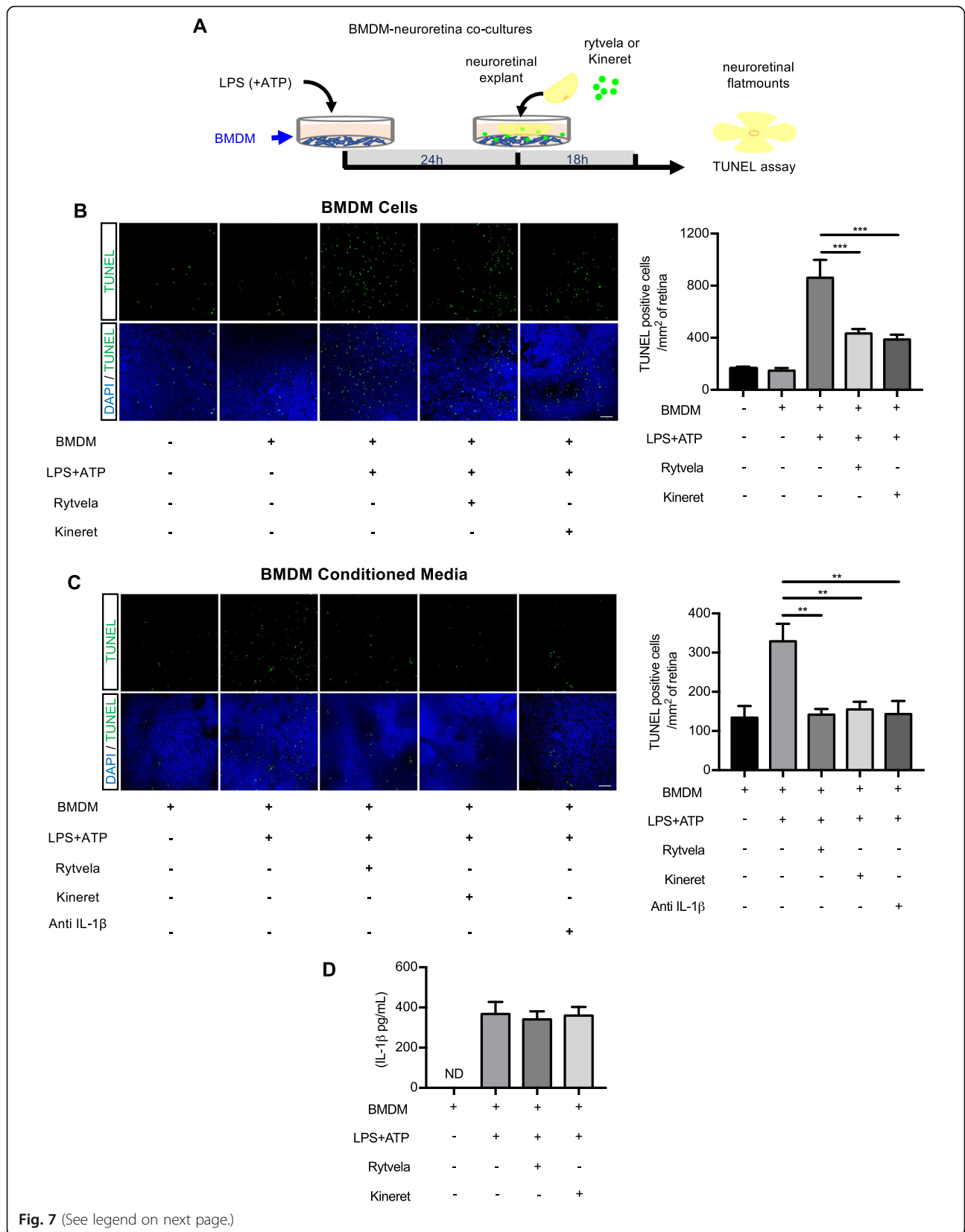


macrophage chemotactic and activating signal (such as through release of DAMPs and chemokines) [79] which would generate IL-1β in MPs; IL-1β would be amplified by IL-1R signaling which can sustain activation of infiltrating MPs while also triggering cell death [32]. Antagonism of IL-1R (with rytvela or Kineret) would arrest this cycle and protect photoreceptors.

Since an important feature in this study applies to the fundamental role of infiltrated MPs that produce IL-1β, which contributes to photoreceptor degeneration, we specifically designed an experiment to show that activated BMDMs (known to generate high levels of IL-1β) or their conditioned media can trigger photoreceptor

death in retinal explants, and is preventable by rytvela and Kineret, which act on IL-1RI-expressing neuroretina without reducing IL-1β concentrations in the BMDM conditioned media.

Using single-cell RNA-seq analysis, we validated that the long-lived pv MFs, which represent a small population of retinal MPs, were the main source of upregulated IL-1β. pv MFs can be defined by their location in contact or close association with the abluminal side of blood vessels [80]. Interestingly, these MPs can migrate from the perivascular space to the photoreceptor layer, participating in retinal degeneration [81].



(See figure on previous page.)

**Fig. 7** Effects of IL-1R inhibition (using rytvela and Kineret) on BMDM-induced photoreceptor toxicity. **a** An illustration of the experimental design used to evaluate the effects of isolated murine bone marrow-derived MPs (BMDMs) stimulated with LPS/ATP (stimulant of IL-1 $\beta$  secretion). **b** TUNEL-stained retinal flat mounts cultured in contact with BMDMs for 18 h in the presence or absence of rytvela or Kineret. Scale bar 50  $\mu$ m. The graph represents the quantification of TUNEL-positive nuclei in the ONL of retinal flat mounts. Data are expressed as mean  $\pm$  SEM and analyzed by one-way ANOVA with Holm-Sidak correction for multiple comparisons;  $n = 5-6$  per group. \*\*\* $p < 0.001$ . **c** TUNEL-stained retinal flat mounts cultured with the conditioned medium of LPS/ATP-activated or not BMDMs in the presence or absence of rytvela, Kineret, or an anti-IL-1 $\beta$  antibody. Scale bar 50  $\mu$ m. The graph represents the quantification of TUNEL-positive nuclei in the ONL of retinal flat mounts. Data are expressed as mean  $\pm$  SEM and analyzed by one-way ANOVA with Holm-Sidak correction for multiple comparisons;  $n = 3-5$  per group. \*\* $p < 0.01$ . **d** ELISA measurement of IL-1 $\beta$  in the conditioned medium derived from BMDMs treated or not with LPS + ATP. The conditioned medium was incubated with retinal explants for 18 h in the presence of vehicle, rytvela, or Kineret.  $n = 4-5$  per group. ND: not detected

Although subretinal MPs are implicated in photoreceptor toxicity via IL-1 $\beta$  secretion, one cannot rule out the involvement of other retinal cell types in modulating inflammation during retinal dystrophies. For instance, IL-1 $\beta$  secreted by infiltrating microglia/macrophages was shown to induce chemokine (Ccl2, Cxcl1, and Cxcl10) expression in Müller and RPE cells implicated in photo-oxidative retinal damage [21]. Conversely, IL-1 $\beta$  inhibition suppressed chemokine expression [21], consistent with our observations. In the mouse retina, we found that *Il1r1* expression was essentially in astrocytes, pericytes, endothelial cells, and bipolar cells. The failure to detect this receptor in MPs and photoreceptors suggests that IL-1 $\beta$ -induced neurotoxicity occurs through other cell type-specific IL-1R1 signaling pathways. One plausible mechanism of this effect might be in part due to the action of IL-1 $\beta$  on astrocytes to trigger glial activation/gliosis. We showed that IL-1R antagonism attenuates retinal gliosis, which is known to cause photoreceptor death. In addition, the action of IL-1 $\beta$  on astrocytes can result in the breakdown of blood-retinal barrier to increase vascular permeability which allows recruitment of MPs to the site of inflammation [82, 83]. Similarly, IL-1 $\beta$  can directly act on pericytes and endothelial cells to disrupt the integrity of blood-retinal barrier [84–87] which in turn, favors vascular permeability. Along these lines, the higher proportion of the short-lived mo MFs in the illuminated retinas suggests a possible disruption of the blood-retinal barrier to allow the infiltration of circulating monocytes [56]. Taken together, phototoxicity releases mediators that attract and stimulate macrophages at the site of injury, which amplify neuroretinal damage via activation of IL-1R. Additional studies are needed to further elucidate the distinct roles of IL-1R in different cell types.

IL-1 $\beta$  plays a complex role which also appears to be concentration-dependent, such that physiologic (low) levels of IL-1 $\beta$  confer protection against photoreceptor degeneration [36, 88]. Low levels of IL-1 $\beta$  enhance production of growth factors [89, 90] such as basic fibroblast growth factor (bFGF), which are relevant to vasculature and photoreceptor protection [21]. Conversely, pathologically elevated levels of IL-1 $\beta$  cause

vascular decay [37, 91, 92]. Despite the evidence pointing toward an important function of IL-1 in photoreceptor death, a previous study has shown that *Il1r1* and *Casp1* deletion was not protective in a light-model of retinal degeneration [93]. However, these results with *Il1r1* knockout animals must be interpreted with caution since compensatory changes may have been adopted during development. In contrast, a more recent study showed that *Caspase-1/11* ablation has a protective role in retinal degeneration [94]. All in all, it is thus reasonable to propose that modulation of IL-1R would be a better alternative to (total) orthosteric antagonism of IL-1R, as the former would bias signaling and induce pharmacological selectivity, whereas the latter would inhibit all signals linked to IL-1R [95]. Along these lines, the allosteric modulator rytvela confers an advantage over orthosteric inhibitors of IL-1R by inhibiting the canonical JNK/p38/c-Jun/AP-1 pathway while preserving NF- $\kappa$ B, which is important for immune vigilance and photoreceptor survival [49, 96, 97]. Accordingly, rytvela protects the choroid and retina from inflammation without displaying adverse effects [33, 91, 98].

In summary, this study pharmacologically validates a major role for IL-1 $\beta$  in triggering neuro-retinal inflammatory responses and neural tissue damage in a model of light-exposed inflammation-triggered neurodegeneration. The development of pharmacologic allosteric IL-1R modulators represents a novel and promising therapeutic approach to tackle retinal degenerative diseases in which IL-1 $\beta$  is implicated. In this context, the advantages of the small peptide rytvela are its superior cytoprotective efficacy and small size compared with current anti-IL-1 therapeutics molecules conferring better distribution [49], ease of administration, low risk of immunogenicity [41], and maintenance of immune vigilance [97].

## Conclusion

Our study implicates an important role of IL-1 $\beta$  signaling in subretinal inflammation and photoreceptor death. We report astroglial and vascular expression of *Il1r1* and that *Il1b* is exclusively upregulated in pv MFs in response to light challenge. Additionally, the IL-1R



modulator *rytvela* confers neuroprotection in photoreceptors following photooxidative stress to the retina. IL-1 receptor modulation is a promising therapeutic avenue to suppress the inflammatory response and preserve photoreceptor integrity in ocular degenerative diseases. It is hoped that our findings will pave the way for future investigations and culminate in clinical trials involving ophthalmic patient populations.

### Supplementary Information

The online version contains supplementary material available at <https://doi.org/10.1186/s12974-020-02032-8>.

**Additional file 1: Supplementary Figure 1.** The absence of colocalization of IL-1R1 with F4/80 in the neuroretina. Representative confocal images showing non-colocalization of IL-1R1 (green) with F4/80+ cells (red).  $n = 4$  per group. Scale bar 20  $\mu\text{m}$ . ONL: outer nuclear layer, INL: inner nuclear layer, GCL: ganglion cell layer.

### Acknowledgements

Not applicable.

### Authors' contributions

RD and SC designed the study. RD planned and directed experiments. RD carried out experiments, assisted by CWHC and PA. RD, GC, and KVS analyzed the data. RD wrote the manuscript. JCR and SC reviewed and edited the manuscript. SO provided scientific advice. JSJ, MD, DO, AGW, and WL provided technical guidance. All authors read and approved the final manuscript.

### Funding

This study was funded by the Canadian Institutes of Health Research (CIHR) grant 950-231837 (SC). RD is supported by Fonds de Recherche du Québec-Santé (FRQS), The Antoine Turmel Foundation, and The Vision Health Research Network. SC holds a Canada Research Chair (Vision Science) and the Leopoldine Wolfe Chair in translational research in age-related macular degeneration.

### Availability of data and materials

All datasets and analyses used in the current study are available from the corresponding author on reasonable request.

### Ethics approval and consent to participate

All animal experiments were approved by the Maisonneuve Rosemont Hospital Animal Care Committee and were performed in accordance with the Association for Research in Vision and Ophthalmology Statement for the Use of Animals in Ophthalmic and Visual Research.

### Consent for publication

Not applicable.

### Competing interests

The corresponding author (SC) holds a patent on a small peptide antagonist of IL-1R, which could be useful in inflammatory ischemic retinopathies, yet this compound remains at the pre-clinical stage and the intellectual property is held by the CHU-Sainte Justine Hospital, Montreal.

### Author details

<sup>1</sup>Department of Pharmacology and Therapeutics, McGill University, Montreal, QC, Canada. <sup>2</sup>Departments of Pediatrics, Ophthalmology, and Pharmacology, Hôpital Maisonneuve-Rosemont Research Center, 5415 Boul L'Assomption, Montreal, QC H1T 2M4, Canada. <sup>3</sup>Hôpital Sainte Justine Research Centre, Montreal, QC, Canada. <sup>4</sup>Department of Obstetrics & Gynecology, University of Alberta, Edmonton, AB, Canada. <sup>5</sup>Department of Neurosurgery, Hôpital Sainte Justine, Montreal, QC, Canada. <sup>6</sup>Department of Chemistry, University of Montreal, Montreal, QC, Canada.

Received: 21 September 2020 Accepted: 10 November 2020

Published online: 27 November 2020

### References

- Xu H, Chen M, Forrester JV. Para-inflammation in the aging retina. *Prog Retin Eye Res.* 2009;28(5):348–68.
- Pfeiffer RL, Marc RE, Jones BW. Persistent remodeling and neurodegeneration in late-stage retinal degeneration. *Prog Retin Eye Res.* 2020;74:100771.
- Clerin E, Marussig M, Sahel JA, Leveillard T. Metabolic and redox signaling of the nucleoredoxin-like-1 gene for the treatment of genetic retinal diseases. *Int J Mol Sci.* 2020;21(5):1625.
- Canto A, Olivar T, Romero FJ, Miranda M. Nitrosative stress in retinal pathologies: review. *Antioxidants (Basel).* 2019;8(11):543.
- Wong WL, Su X, Li X, Cheung CM, Klein R, Cheng CY, et al. Global prevalence of age-related macular degeneration and disease burden projection for 2020 and 2040: a systematic review and meta-analysis. *Lancet Glob Health.* 2014;2(2):e106–16.
- Coleman HR, Chan CC, Ferris FL 3rd, Chew EY. Age-related macular degeneration. *Lancet.* 2008;372(9652):1835–45.
- Combadiere C, Feumi C, Raoul W, Keller N, Rodero M, Pezard A, et al. CX3CR1-dependent subretinal microglia cell accumulation is associated with cardinal features of age-related macular degeneration. *J Clin Invest.* 2007;117(10):2920–8.
- Gupta N, Brown KE, Milam AH. Activated microglia in human retinitis pigmentosa, late-onset retinal degeneration, and age-related macular degeneration. *Exp Eye Res.* 2003;76(4):463–71.
- Haines JL, Hauser MA, Schmidt S, Scott WK, Olson LM, Gallins P, et al. Complement factor H variant increases the risk of age-related macular degeneration. *Science.* 2005;308(5720):419–21.
- Klein RJ, Zeiss C, Chew EY, Tsai JY, Sackler RS, Haynes C, et al. Complement factor H polymorphism in age-related macular degeneration. *Science.* 2005;308(5720):385–9.
- Wooff Y, Man SM, Aggio-Bruce R, Natoli R, Fernando N. IL-1 Family members mediate cell death, inflammation and angiogenesis in retinal degenerative diseases. *Front Immunol.* 2019;10:1618.
- Mellal K, Omri S, Mulumba M, Tahiri H, Fortin C, Dorion MF, et al. Immunometabolic modulation of retinal inflammation by CD36 ligand. *Sci Rep.* 2019;9(1):12903.
- Rozing MP, Durhuus JA, Krogh Nielsen M, Subhi Y, Kirkwood TB, Westendorp RG, et al. Age-related macular degeneration: a two-level model hypothesis. *Prog Retin Eye Res.* 2019;76:100825.
- Damani MR, Zhao L, Fontainhas AM, Amaral J, Fariss RN, Wong WT. Age-related alterations in the dynamic behavior of microglia. *Aging Cell.* 2011;10(2):263–76.
- Cruz-Guilloty F, Saeed AM, Echeagaray JJ, Duffort S, Ballmick A, Tan Y, et al. Infiltration of proinflammatory m1 macrophages into the outer retina precedes damage in a mouse model of age-related macular degeneration. *Int J Inflamm.* 2013;2013:503725.
- Whitcup SM, Nussenblatt RB, Lightman SL, Hollander DA. Inflammation in retinal disease. *Int J Inflamm.* 2013;2013:724648.
- Guillonneau X, Eandi CM, Paques M, Sahel JA, Sapiéha P, Sennlaub F. On phagocytes and macular degeneration. *Prog Retin Eye Res.* 2017;61:98–128.
- Lavalette S, Conart JB, Touhami S, Roubeix C, Houssier M, Augustin S, et al. CD36 deficiency inhibits retinal inflammation and retinal degeneration in Cx3cr1 knockout mice. *Front Immunol.* 2019;10:3032.
- Block ML, Zecca L, Hong JS. Microglia-mediated neurotoxicity: uncovering the molecular mechanisms. *Nat Rev Neurosci.* 2007;8(1):57–69.
- Zhao M, Bai Y, Xie W, Shi X, Li F, Yang F, et al. Interleukin-1beta level is increased in vitreous of patients with neovascular age-related macular degeneration (nAMD) and polypoidal choroidal vasculopathy (PCV). *PLoS One.* 2015;10(5):e0125150.
- Natoli R, Fernando N, Madigan M, Chu-Tan JA, Valter K, Provis J, et al. Microglia-derived IL-1beta promotes chemokine expression by Muller cells and RPE in focal retinal degeneration. *Mol Neurodegener.* 2017;12(1):31.
- Kataoka K, Matsumoto H, Kaneko H, Notomi S, Takeuchi K, Sweigard JH, et al. Macrophage- and RIP3-dependent inflammasome activation exacerbates retinal detachment-induced photoreceptor cell death. *Cell Death Dis.* 2015;6:e1731.

23. Eandi CM, Charles Messance H, Augustin S, Dominguez E, Lavalette S, Forster V, et al. Subretinal mononuclear phagocytes induce cone segment loss via IL-1beta. *Elife*. 2016;5:e16490.
24. Tarallo V, Hirano Y, Gelfand Bradley D, Dridi S, Kerur N, Kim Y, et al. DICER1 loss and Alu RNA induce age-related macular degeneration via the NLRP3 inflammasome and MyD88. *Cell*. 2012;149(4):847–59.
25. Doyle SL, Campbell M, Ozaki E, Salomon RG, Mori A, Kenna PF, et al. NLRP3 has a protective role in age-related macular degeneration through the induction of IL-18 by drusen components. *Nat Med*. 2012;18(5):791–8.
26. Munoz-Planillo R, Kuffa P, Martinez-Colon G, Smith BL, Rajendiran TM, Nunez G. K(+) efflux is the common trigger of NLRP3 inflammasome activation by bacterial toxins and particulate matter. *Immunity*. 2013;38(6):1142–53.
27. Mariathasan S, Weiss DS, Newton K, McBride J, O'Rourke K, Roose-Girma M, et al. Cryopyrin activates the inflammasome in response to toxins and ATP. *Nature*. 2006;440(7081):228–32.
28. Gross O, Yazdi AS, Thomas CJ, Masin M, Heinz LX, Guarda G, et al. Inflammasome activators induce interleukin-1alpha secretion via distinct pathways with differential requirement for the protease function of caspase-1. *Immunity*. 2012;36(3):388–400.
29. Gao J, Cui JZ, To E, Cao S, Matsubara JA. Evidence for the activation of pyroptotic and apoptotic pathways in RPE cells associated with NLRP3 inflammasome in the rodent eye. *J Neuroinflammation*. 2018;15(1):15.
30. Brandstetter C, Patt J, Holz FG, Krohne TU. Inflammasome priming increases retinal pigment epithelial cell susceptibility to lipofuscin phototoxicity by changing the cell death mechanism from apoptosis to pyroptosis. *J Photochem Photobiol B*. 2016;161:177–83.
31. Newman AM, Gallo NB, Hancox LS, Miller NJ, Radeke CM, Maloney MA, et al. Systems-level analysis of age-related macular degeneration reveals global biomarkers and phenotype-specific functional networks. *Genome Med*. 2012;4(2):16.
32. Hu SJ, Calippe B, Lavalette S, Roubeix C, Montassar F, Housset M, et al. Upregulation of P2RX7 in Cx3cr1-Deficient mononuclear phagocytes leads to increased interleukin-1beta secretion and photoreceptor neurodegeneration. *J Neurosci*. 2015;35(18):6987–96.
33. Rivera JC, Sitaras N, Noueihed B, Hamel D, Madaan A, Zhou T, et al. Microglia and interleukin-1beta in ischemic retinopathy elicit microvascular degeneration through neuronal semaphorin-3A. *Arterioscler Thromb Vasc Biol*. 2013;33(8):1881–91.
34. Guadagno J, Swan P, Shaikh R, Cregan SP. Microglia-derived IL-1beta triggers p53-mediated cell cycle arrest and apoptosis in neural precursor cells. *Cell Death Dis*. 2015;6:e1779.
35. Zhao L, Zabel MK, Wang X, Ma W, Shah P, Fariss RN, et al. Microglial phagocytosis of living photoreceptors contributes to inherited retinal degeneration. *EMBO Mol Med*. 2015;7(9):1179–97.
36. LaVail MM, Unoki K, Yasumura D, Matthes MT, Yancopoulos GD, Steinberg RH. Multiple growth factors, cytokines, and neurotrophins rescue photoreceptors from the damaging effects of constant light. *Proc Natl Acad Sci U S A*. 1992;89(23):11249–53.
37. Lavalette S, Raoul W, Houssier M, Camelo S, Levy O, Calippe B, et al. Interleukin-1beta inhibition prevents choroidal neovascularization and does not exacerbate photoreceptor degeneration. *Am J Pathol*. 2011;178(5):2416–23.
38. Dinarello CA. Overview of the IL-1 family in innate inflammation and acquired immunity. *Immunol Rev*. 2018;281(1):8–27.
39. Colotta F, Re F, Muzio M, Bertini R, Polentarutti N, Sironi M, et al. Interleukin-1 type II receptor: a decoy target for IL-1 that is regulated by IL-4. *Science*. 1993;261(5120):472–5.
40. Braddock M, Quinn A, Canvin J. Therapeutic potential of targeting IL-1 and IL-18 in inflammation. *Expert Opin Biol Ther*. 2004;4(6):847–60.
41. Quiniou C, Sapiéha P, Lahaie I, Hou X, Brault S, Beauchamp M, et al. Development of a novel noncompetitive antagonist of IL-1 receptor. *J Immunol*. 2008;180(10):6977–87.
42. McDonnell JM, Beavil AJ, Mackay GA, Jameson BA, Korngold R, Gould HJ, et al. Structure based design and characterization of peptides that inhibit IgE binding to its high-affinity receptor. *Nat Struct Biol*. 1996;3(5):419–26.
43. Smith JS, Lefkowitz RJ, Rajagopal S. Biased signalling: from simple switches to allosteric microprocessors. *Nat Rev Drug Discov*. 2018;17(4):243–60.
44. Tuttle AH, Philip VM, Chesler EJ, Mogil JS. Comparing phenotypic variation between inbred and outbred mice. *Nat Methods*. 2018;15(12):994–6.
45. Mukaratirwa S, Petterino C, Naylor SW, Bradley A. Incidences and range of spontaneous lesions in the eye of Cr1:CD-1(ICR)BR mice used in toxicity studies. *Toxicol Pathol*. 2015;43(4):530–5.
46. Butler A, Hoffman P, Smibert P, Papalex E, Satija R. Integrating single-cell transcriptomic data across different conditions, technologies, and species. *Nat Biotechnol*. 2018;36(5):411–20.
47. Heng JS, Hackett SF, Stein-O'Brien GL, Winer BL, Williams J, Goff LA, et al. Comprehensive analysis of a mouse model of spontaneous uveoretinitis using single-cell RNA sequencing. *Proc Natl Acad Sci U S A*. 2019; 116(52): 26734–44.
48. O'Koren EG, Yu C, Klingeborn M, AYW W, Prigge CL, Mathew R, et al. Microglial function is distinct in different anatomical locations during retinal homeostasis and degeneration. *Immunity*. 2019;50(3):723–37 e7.
49. Nadeau-Vallee M, Quiniou C, Palacios J, Hou X, Erfani A, Madaan A, et al. Novel noncompetitive IL-1 receptor-biased ligand prevents infection- and inflammation-induced preterm birth. *J Immunol*. 2015;195(7):3402–15.
50. Lewis GP, Matsumoto B, Fisher SK. Changes in the organization and expression of cytoskeletal proteins during retinal degeneration induced by retinal detachment. *Invest Ophthalmol Vis Sci*. 1995;36(12):2404–16.
51. Luna G, Lewis GP, Banna CD, Skalli O, Fisher SK. Expression profiles of nestin and synemin in reactive astrocytes and Muller cells following retinal injury: a comparison with glial fibrillar acidic protein and vimentin. *Mol Vis*. 2010;16: 2511–23.
52. de Raad S, Szczesny PJ, Munz K, Reme CE. Light damage in the rat retina: glial fibrillary acidic protein accumulates in Muller cells in correlation with photoreceptor damage. *Ophthalmic Res*. 1996;28(2):99–107.
53. Stoffels M, Zaal R, Kok N, van der Meer JW, Dinarello CA, Simon A. ATP-induced IL-1beta specific secretion: true under stringent conditions. *Front Immunol*. 2015;6:54.
54. Heneka MT, Kummer MP, Latz E. Innate immune activation in neurodegenerative disease. *Nat Rev Immunol*. 2014;14(7):463–77.
55. Rutar M, Natoli R, Provis JM. Small interfering RNA-mediated suppression of Ccl2 in Muller cells attenuates microglial recruitment and photoreceptor death following retinal degeneration. *J Neuroinflammation*. 2012;9:221.
56. Sennlaub F, Auvynet C, Calippe B, Lavalette S, Poupel L, Hu SJ, et al. CCR2(+) monocytes infiltrate atrophic lesions in age-related macular disease and mediate photoreceptor degeneration in experimental subretinal inflammation in Cx3cr1 deficient mice. *EMBO Mol Med*. 2013;5(11):1775–93.
57. Nassar K, Grisanti S, Elfar E, Luke J, Luke M, Grisanti S. Serum cytokines as biomarkers for age-related macular degeneration. *Graefes Arch Clin Exp Ophthalmol*. 2015;253(5):699–704.
58. Hu Z, Zhang Y, Wang J, Mao P, Lv X, Yuan S, et al. Knockout of Ccr2 alleviates photoreceptor cell death in rodent retina exposed to chronic blue light. *Cell Death Dis*. 2016;7(11):e2468.
59. Heneka MT, Kummer MP, Stutz A, Delekate A, Schwartz S, Vieira-Saecker A, et al. NLRP3 is activated in Alzheimer's disease and contributes to pathology in APP/PS1 mice. *Nature*. 2013;493(7434): 674–8.
60. Lucas SM, Rothwell NJ, Gibson RM. The role of inflammation in CNS injury and disease. *Br J Pharmacol*. 2006;147(Suppl 1):S232–40.
61. Koprach JB, Reske-Nielsen C, Mithal P, Isacson O. Neuroinflammation mediated by IL-1beta increases susceptibility of dopamine neurons to degeneration in an animal model of Parkinson's disease. *J Neuroinflammation*. 2008;5:8.
62. Italiani P, Puxeddu I, Napoletano S, Scala E, Melillo D, Manocchio S, et al. Circulating levels of IL-1 family cytokines and receptors in Alzheimer's disease: new markers of disease progression? *J Neuroinflammation*. 2018; 15(1):342.
63. Allan SM, Tyrrell PJ, Rothwell NJ. Interleukin-1 and neuronal injury. *Nat Rev Immunol*. 2005;5(8):629–40.
64. Grimm C, Reme CE. Light damage as a model of retinal degeneration. *Methods Mol Biol*. 2013;935:87–97.
65. Nakamura M, Kuse Y, Tsuruma K, Shimazawa M, Hara H. The involvement of the oxidative stress in murine blue LED light-induced retinal damage model. *Biol Pharm Bull*. 2017;40(8):1219–25.
66. Galea I, Bechmann I, Perry VH. What is immune privilege (not)? *Trends Immunol*. 2007;28(1):12–8.
67. Levy O, Calippe B, Lavalette S, Hu SJ, Raoul W, Dominguez E, et al. Apolipoprotein E promotes subretinal mononuclear phagocyte survival and chronic inflammation in age-related macular degeneration. *EMBO Mol Med*. 2015;7(2):211–26.
68. Westman J, Grinstein S, Marques PE. Phagocytosis of necrotic debris at sites of injury and inflammation. *Front Immunol*. 2019;10:3030.

69. Chen H, Liu B, Lukas TJ, Neufeld AH. The aged retinal pigment epithelium/choroid: a potential substratum for the pathogenesis of age-related macular degeneration. *PLoS One*. 2008;3(6):e2339.
70. Dharmarajan S, Fisk DL, Sorenson CM, Sheibani N, Belecky-Adams TL. Microglia activation is essential for BMP7-mediated retinal reactive gliosis. *J Neuroinflammation*. 2017;14(1):76.
71. Bringmann A, Iandiev I, Pannicke T, Wurm A, Hollborn M, Wiedemann P, et al. Cellular signaling and factors involved in Muller cell gliosis: neuroprotective and detrimental effects. *Prog Retin Eye Res*. 2009;28(6):423–51.
72. Nakazawa T, Takeda M, Lewis GP, Cho KS, Jiao J, Wilhelmsson U, et al. Attenuated glial reactions and photoreceptor degeneration after retinal detachment in mice deficient in glial fibrillary acidic protein and vimentin. *Invest Ophthalmol Vis Sci*. 2007;48(6):2760–8.
73. Tschopp J, Schroder K. NLRP3 inflammasome activation: the convergence of multiple signalling pathways on ROS production? *Nat Rev Immunol*. 2010;10(3):210–5.
74. Portillo JC, Lopez Corcino Y, Miao Y, Tang J, Sheibani N, Kern TS, et al. CD40 in retinal muller cells induces P2X7-dependent cytokine expression in macrophages/microglia in diabetic mice and development of early experimental diabetic retinopathy. *Diabetes*. 2017;66(2):483–93.
75. Gentle IE, McHenry KT, Weber A, Metz A, Kretz O, Porter D, et al. TIR-domain-containing adapter-inducing interferon-beta (TRIF) forms filamentous structures, whose pro-apoptotic signalling is terminated by autophagy. *FEBS J*. 2017;284(13):1987–2003.
76. Wang JJ, Williams W, Wang B, Wei J, Lu X, Cheng JW, et al. Cytotoxic effect of interleukin-8 in retinal ganglion cells and its possible mechanisms. *Int J Ophthalmol*. 2018;11(8):1277–83.
77. Charles-Messance H, Blot G, Couturier A, Vignaud L, Touhami S, Beguier F, et al. IL-1beta induces rod degeneration through the disruption of retinal glutamate homeostasis. *J Neuroinflammation*. 2020;17(1):1.
78. Yasuhara R, Miyamoto Y, Akaike T, Akuta T, Nakamura M, Takami M, et al. Interleukin-1beta induces death in chondrocyte-like ATDC5 cells through mitochondrial dysfunction and energy depletion in a reactive nitrogen and oxygen species-dependent manner. *Biochem J*. 2005;389(Pt 2):315–23.
79. Garg AD, Nowis D, Golab J, Agostinis P. Photodynamic therapy: illuminating the road from cell death towards anti-tumour immunity. *Apoptosis*. 2010;15(9):1050–71.
80. Lapenna A, De Palma M, Lewis CE. Perivascular macrophages in health and disease. *Nat Rev Immunol*. 2018;18(11):689–702.
81. Mendes-Jorge L, Ramos D, Luppo M, Llombart C, Alexandre-Pires G, Nacher V, et al. Scavenger function of resident autofluorescent perivascular macrophages and their contribution to the maintenance of the blood-retinal barrier. *Invest Ophthalmol Vis Sci*. 2009;50(12):5997–6005.
82. Argaw AT, Asp L, Zhang J, Navrazhina K, Pham T, Mariani JN, et al. Astrocyte-derived VEGF-A drives blood-brain barrier disruption in CNS inflammatory disease. *J Clin Invest*. 2012;122(7):2454–68.
83. Argaw AT, Zhang Y, Snyder BJ, Zhao ML, Kopp N, Lee SC, et al. IL-1beta regulates blood-brain barrier permeability via reactivation of the hypoxia-angiogenesis program. *J Immunol*. 2006;177(8):5574–84.
84. Luna JD, Chan CC, Derevjaniuk NL, Mahlow J, Chiu C, Peng B, et al. Blood-retinal barrier (BRB) breakdown in experimental autoimmune uveoretinitis: comparison with vascular endothelial growth factor, tumor necrosis factor alpha, and interleukin-1beta-mediated breakdown. *J Neurosci Res*. 1997;49(3):268–80.
85. Skaria T, Bachli E, Schoedon G. Wnt5A/Ryk signaling critically affects barrier function in human vascular endothelial cells. *Cell Adhes Migr*. 2017;11(1):24–38.
86. Daneman R, Zhou L, Kebede AA, Barres BA. Pericytes are required for blood-brain barrier integrity during embryogenesis. *Nature*. 2010;468(7323):562–6.
87. Persidsky Y, Hill J, Zhang M, Dykstra H, Winfield M, Reichenbach NL, et al. Dysfunction of brain pericytes in chronic neuroinflammation. *J Cereb Blood Flow Metab*. 2016;36(4):794–807.
88. Whiteley SJ, Klassen H, Coffey PJ, Young MJ. Photoreceptor rescue after low-dose intravitreal IL-1beta injection in the RCS rat. *Exp Eye Res*. 2001;73(4):557–68.
89. Mantovani A, Bussoloni F, Dejana E. Cytokine regulation of endothelial cell function. *FASEB J*. 1992;6(8):2591–9.
90. Carmi Y, Voronov E, Dotan S, Lahat N, Rahat MA, Fogel M, et al. The role of macrophage-derived IL-1 in induction and maintenance of angiogenesis. *J Immunol*. 2009;183(7):4705–14.
91. Beaudry-Richard A, Nadeau-Vallee M, Prairie E, Maurice N, Heckel E, Nezhady M, et al. Antenatal IL-1-dependent inflammation persists postnatally and causes retinal and sub-retinal vasculopathy in progeny. *Sci Rep*. 2018;8(1):11875.
92. Zhou TE, Rivera JC, Bhosle VK, Lahaie I, Shao Z, Tahiri H, et al. Choroidal involution is associated with a progressive degeneration of the outer retinal function in a model of retinopathy of prematurity: early role for IL-1beta. *Am J Pathol*. 2016;186(12):3100–16.
93. Samardzija M, Wenzel A, Thiersch M, Frigg R, Reme C, Grimm C. Caspase-1 ablation protects photoreceptors in a model of autosomal dominant retinitis pigmentosa. *Invest Ophthalmol Vis Sci*. 2006;47(12):5181–90.
94. Wooff Y, Fernando N, Wong JHC, Dietrich C, Aggio-Bruce R, Chu-Tan JA, et al. Caspase-1-dependent inflammasomes mediate photoreceptor cell death in photo-oxidative damage-induced retinal degeneration. *Sci Rep*. 2020;10(1):2263.
95. Kenakin T. Principles: receptor theory in pharmacology. *Trends Pharmacol Sci*. 2004;25(4):186–92.
96. Yang LP, Zhu XA, Tso MO. Role of NF-kappaB and MAPKs in light-induced photoreceptor apoptosis. *Invest Ophthalmol Vis Sci*. 2007;48(10):4766–76.
97. Sayah DN, Zhou TE, Omri S, Mazzaferri J, Quiniou C, Wirth M, et al. Novel anti-interleukin-1beta Therapy preserves retinal integrity: a longitudinal investigation using OCT imaging and automated retinal segmentation in small rodents. *Front Pharmacol*. 2020;11:296.
98. Geranurimi A, Cheng CWH, Quiniou C, Zhu T, Hou X, Rivera JC, et al. Probing Anti-inflammatory properties independent of NF-kappaB through conformational constraint of peptide-based interleukin-1 receptor biased ligands. *Front Chem*. 2019;7:23.

## Publisher's Note

Springer Nature remains neutral with regard to jurisdictional claims in published maps and institutional affiliations.

**Ready to submit your research? Choose BMC and benefit from:**

- fast, convenient online submission
- thorough peer review by experienced researchers in your field
- rapid publication on acceptance
- support for research data, including large and complex data types
- gold Open Access which fosters wider collaboration and increased citations
- maximum visibility for your research: over 100M website views per year

**At BMC, research is always in progress.**

Learn more [biomedcentral.com/submissions](https://biomedcentral.com/submissions)

